Simulation of the Summer Monsoon over India in the Ensemble of Seasonal Simulations from the ECMWF Reanalyzed Data

B. K. BASU

NCMRWF, Mausam Bhavan Complex, New Delhi, India

(Manuscript received in final form 6 May 1999)

ABSTRACT

The ensemble of seasonal (120 days) simulations of the Northern Hemispheric summer for the reanalysis period of the European Centre for Medium-Range Weather Forecasts has been examined to assess the extent to which the characteristic features of the Indian summer monsoon can be reproduced in these simulations. The present simulations could reproduce a better distribution of the seasonal average precipitation over India in comparison with the earlier Atmospheric Model Intercomparison Project simulations. The interannual variation in the seasonal total of the spatially averaged precipitation over India has predictability. The 10-day-average precipitation values did not show any impact of the El Niño or La Niña events or any periodicity in the amount of precipitation. The intraseasonal variability did not produce any distinct pattern for 10-day-average rainfall during the excess or deficient years. The simulated patterns over India correspond to the weak phase of summer monsoon with excess precipitation over the northeastern part of the country and adjoining China. The cloud cover is less over the central parts of India and near-ground maximum temperature is higher. A simulated motion field reproduces the typical features of the Indian summer monsoon including the low-frequency seasonal migration of the Tibetan anticyclone at 200 hPa.

1. Introduction

In any numerical weather prediction center the forecast model and the data assimilation system usually undergo changes over the years. Since, a homogeneous multiyear sequence of analyses is required to prepare the climate as simulated by the analysis-forecast system, to study the interannual and intra-annual variabilities, for model validation and also for various diagnostic studies, a need for the reanalysis of past data with a fixed state-of-the-art model and analysis system was felt by the modeling community. An added advantage is the maximization of data by including the information that might have been missed earlier due to the operational requirement of a cutoff time limit or due to any other reason. Recently the reanalysis for varying periods of time have been completed by the European Centre for Medium-Range Weather Forecasts (ECMWF; 1979–93), the National Centers for Environmental Prediction (1947–96), and the National Aeronautics and Space Administration Goddard Space Flight Center (1985–93). Recent evaluation of the ECMWF reanalysis data (Hoinka 1998) has shown improvement in the trends in total pressure and water vapor pressure. Using this reanalyzed data as input, ECMWF has produced a 9-member ensemble of seasonal (120 days) simulations for each season of the 15 years and distributed 10-day means of these output for evaluation. In the present work some characteristic features of these simulations, over the Indian region, have been derived for the summer monsoon period covering 120 days from 1 June and compared with observations available from the India Meteorological Department (IMD)

The forecast model used for the seasonal simulations at ECMWF was the T63L31 version of the Integrated Forecast System (IFS) and the output was processed to produce surface and upper-air fields at an uniform resolution of 2.5° in latitude and longitude. The 9-member ensemble are generated by using the initial conditions that lead the target date by 9–1 days, successively, that is, for the summer season the first member of the ensemble starts with the 1200 UTC initial condition of 23 May, while the ninth member starts with the 1200 UTC initial condition of 31 May. All ensembles had the same sea surface temperature (the U.K. Met. Office Global Sea-Ice and SST data up to 1981 and Reynolds Optimally Interpolated analysis after that) updated daily. The output contains selected surface fields as well as upper-air fields at a few specific pressure levels. The 10-day-averages of 1-day forecasts of the same fields were also provided at the same resolution. For those variables for which observations are difficult to obtain, these average 1-day forecasts are used as a benchmark for comparison.

Corresponding author address: Dr. B. K. Basu, NCMRWF, Mausam Bhavan Complex, Lodi Road, New Delhi 110 003 India.
E-mail: bkbasu@ncmrwf.gov.in

The reanalysis project at ECMWF has used the METEOSAT data over the Indian Ocean in 1979 and after 1983, and mostly wind data from the upper-air observation over India.

2. Methodology

The Indian summer monsoon has some definite characteristics (Rao 1976) in the distribution of surface fields like precipitation, mean sea level pressure, surface temperature, etc., as well as the circulation and thermodynamic features of the lower, mid-, and upper troposphere. A long series of observations, extending well over a century, is available over a large number of surface and upper-air observatories fairly distributed over India, and long-term averages constituting the climate of India are also available for 30-yr periods, the latest being that for the period 1951–80. A climate diagnostic bulletin is also being prepared by IMD for the past few years to assess the interannual variations in the monthly and seasonal mean features over India. These observed climatological fields have been used for comparisons with the 15-yr averages of the verifying and simulated fields over India during the monsoon season.

It is well known that each numerical weather prediction model produces its own climate when integrated over a long period far exceeding the limit of dynamic predictability. Such models produced climates that vary from each other and also from the observed climate itself. Since 135 simulations of the Indian summer monsoon are available for 15 yr between 1979 and 1993, an average of these simulations have been formed to represent the climate of the T63L31 version of the IFS model used to produce these simulations. This simulated model climate has been compared with the observed values over India as well as the 15-yr mean of 1-day forecasts to determine the extent of systematic differences in the simulated climate over India.

The interannual variability in the Indian summer monsoon rainfall and its dependence on the ENSO phenomena (Shukla 1991) has been of interest to the international community of atmospheric scientists and the extreme variability between scanty and abundant rainfall over India during the years 1987 and 1988, respectively, was the target for simulation during the Monsoon Numerical Experimentation Group experiment. Though only a part of the Indian monsoon variability could be explained by the changes in sea surface temperatures (Kar and Basu 1992), the necessity of ensembles of simulations for a more reliable prediction (Palmer et al. 1992) was understood during this experiment. In the present work the intra- and interannual variations in simulated precipitation are studied by computing the spatial average over the Indian area as shown in Fig. 1.

In addition to precipitation, the other fields available in the CD-ROM are the mean sea level pressure, total cloud cover, near-surface temperatures, components of radiation budget, circulation at the lower (850 hPa) and upper (200 hPa) troposphere, temperatures at the lower, mid- (500 hPa), and upper troposphere, and vertical velocity at the midtroposphere. For most of these parameters the difference of the seasonal mean of 135 simulations from the mean verifying 1-day prediction was computed to determine the seasonal tendencies in the simulations. The decadal averages were also examined to determine the intraseasonal variability and presence of slowly varying modes.

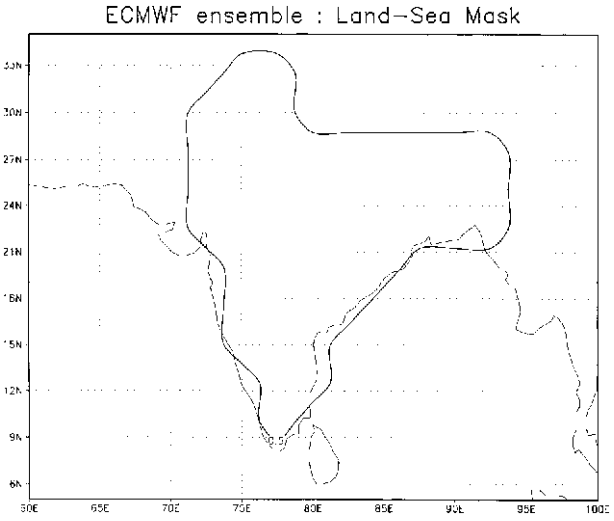

FIG. 1. Area of spatial averaging over India.

3. Spatial and temporal distribution of precipitation over India in the seasonal simulations of the southwest monsoon

During the southwest monsoon (1 June–30 September) the seasonal precipitation has some typical features (Rao 1976) that are reproduced in the medium-range predictions by many of the operational numerical weather prediction centers (Basu et al. 1999). When averaged over the 15 years of the reanalysis period, the 1-day predictions produce a spatial distribution of seasonal mean as shown in Fig. 2. Copius precipitation along the west coast with values exceeding 160 cm and the strong west to east decrease, leading to values less than 20 cm along the east coast, agree well with the normal values prepared by the IMD from 1951–80 observations. The scanty amounts over the northwestern deserts and the second belt of heavy rainfall to the east and northeast of the country are also well represented in the mean 1-day predictions.

In the mean seasonal simulation, the accumulated precipitation amounts are less than the 15-yr mean 1-day precipitation amounts over most of India with a maximum deficit exceeding 80 cm (Fig. 3) along the west coast. An area of excess rain is noticed over the northeastern part of India and adjoining countries. A comparison with the geographical feature shows that both

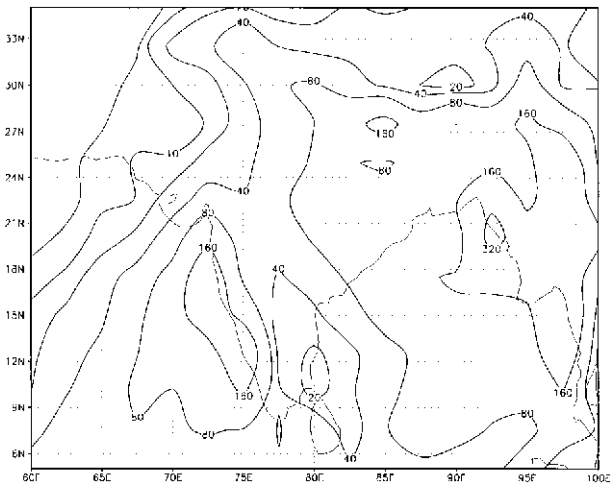

FIG. 2. Seasonal total precipitation (cm) from 1-day forecasts averaged over 15 yr (1979–93).

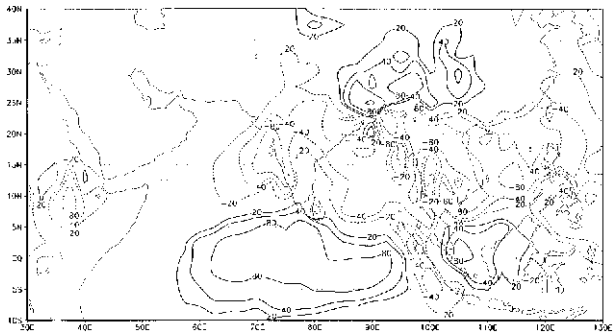

FIG. 3. Difference between the mean simulated and mean verifying 1-day precipitation (seasonal total; cm).

the areas of maximum deficit and excess in precipitation are in the proximity of hill ranges of low elevation (~1 km). An examination of the near-surface wind flow may reveal whether the mean seasonal simulation has a weaker (stronger) cross-mountain component near the deficit (excess) rainfall area. The decrease in rainfall over the rest of India indicates a weakening of the monsoon system in the simulations. During the strong monsoon epochs over India, the low-level wind turns cyclonically over the head bay and transports moisture into the central plains of India, while during the weak monsoon epochs the moist air flows across the northeast of India into the southwestern parts of China where rainfall amounts increase significantly. This oscillation of precipitation maximum between the Indian and Chinese regions has been described by Congbin and Fan (1984) and corresponds to the first principal component of the variation in monthly mean precipitation over India (B. Mukhopadhyay 1998, personal communication).

Another important feature noticed in the mean simulation is the increase in rainfall over the equatorial convergence zone compared to that in the mean 1-day verifying predictions. This locking of the rainfall over the oceanic mode, at the cost of the mode over land was also noticed in the Atmospheric Model Intercomparison Project (AMIP) simulations (Gadgil et al. 1998). However, the rainfall belt between 20° and 30°N over land is much better reproduced and extends almost up to 80°E in the present simulations compared to 90°E in the AMIP simulation. Better resolution (T63L31) and improved physical parameterizations of the forecast model used in this simulation experiment, compared to that (T42L19) in the AMIP experiment, may be some of the reasons for this improvement.

The total precipitation over India as a whole is computed by the IMD on a weekly basis (Thursday to Wednesday) as a part of its operational schedule. This is a single value obtained by taking arithmetic mean of about 2000 observations distributed over India. The observatory network varies slightly from week to week due to operational constraint as observations arriving after the cutoff time cannot be included in the computation. The seasonal total and its departure from normal are computed at the end of the season (Table 1). A comparison of the observed departures of the seasonal total with similar departures computed from the 1-day predictions is presented in Fig. 4. The mean Indian precipitation for the monsoon period in a particular year is taken to be normal when the departure lies within one standard deviation (9%) on either side of the normal. For the verifying prediction a value of 85 cm has been taken as the average seasonal total for the whole of India. It is seen that the interannual trend in the seasonal total was captured in the 1-day predictions except in 1981 and 1984 when small deficits were predicted as small excesses. When a comparison is made on the basis of the three categories of excess, normal, and deficient, the predictions for the years 1980, 1982, 1990, and 1992

TABLE 1. Area-weighted rainfall for India as a whole (monsoon season; mm). Normal value changes from one year to another as the number of precipitation gauges in the network varies. Accurate value for percent departure is not available for 1979 though the category is known to be deficient.

Year	Actual	Normal	% departure	Category
1980	896.1	858.2	+4	Normal
1981	830.5	858.5	−3	Normal
1982	761.1	872.0	−13	Deficient
1983	986.0	880.1	+12	Excess
1984	838.8	906.5	−7	Normal
1985	863.3	936.9	−6	Normal
1986	758.0	900.3	−16	Deficient
1987	731.0	924.9	−21	Deficient
1988	1107.2	940.4	+18	Excess
1989	897.0	884.0	+1	Normal
1990	935.9	881.4	+6	Normal
1991	815.0	881.0	−7	Normal
1992	831.0	899.0	−7	Normal
1993	902.0	909.0	−1	Normal
1994	1001.0	907.0	+10	Excess
1995	904.0	908.0	0	Normal
1996	935.0	905.7	+3	Normal
1997	832.4	891.7	−7	Normal

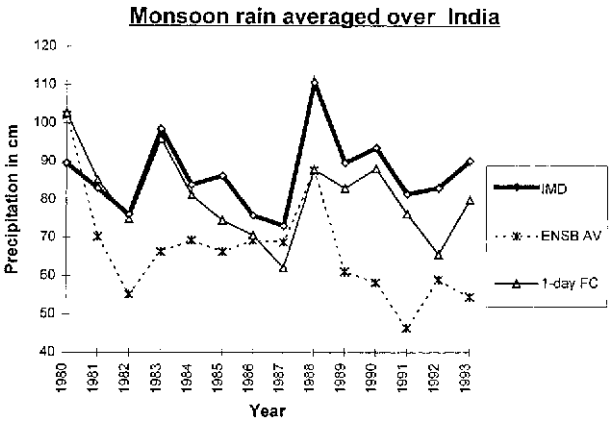

FIG. 4. Mean Indian precipitation (cm) computed from observed (IMD), 1-day forecasts, ensemble average of simulations, and standardized ensemble average.

differ from the verifying by one category. The large variability in rainfall between 1987 and 1988 is also reproduced well in the seasonal mean 1-day predictions. The ability of the ECMWF model to simulate the interannual variability has been reported by Sperber and Palmer (1996) and Gadgil et al. (1998).

The accumulated seasonal precipitation in the simulations, when compared to the seasonal total of predicted 1-day precipitation, shows lower values for almost all the simulations irrespective of the years and starting date of the simulation. As seen in Fig. 5a, there are only a few simulations that show total seasonal precipitation in excess of the verifying predictions and most of these correspond to the two deficient years of 1979 and 1987. There is no indication that a set of simulations with a particular lead time, that is, starting on a particular date, show any definite pattern when compared to the verifying predictions. Similarly no particular pattern could be discerned for the El Niño years of 1982, 1987, and 1992 or the La Niña years of 1984 and 1988.

The seasonal totals of simulated precipitation, averaged over India, has been standardized to have the same

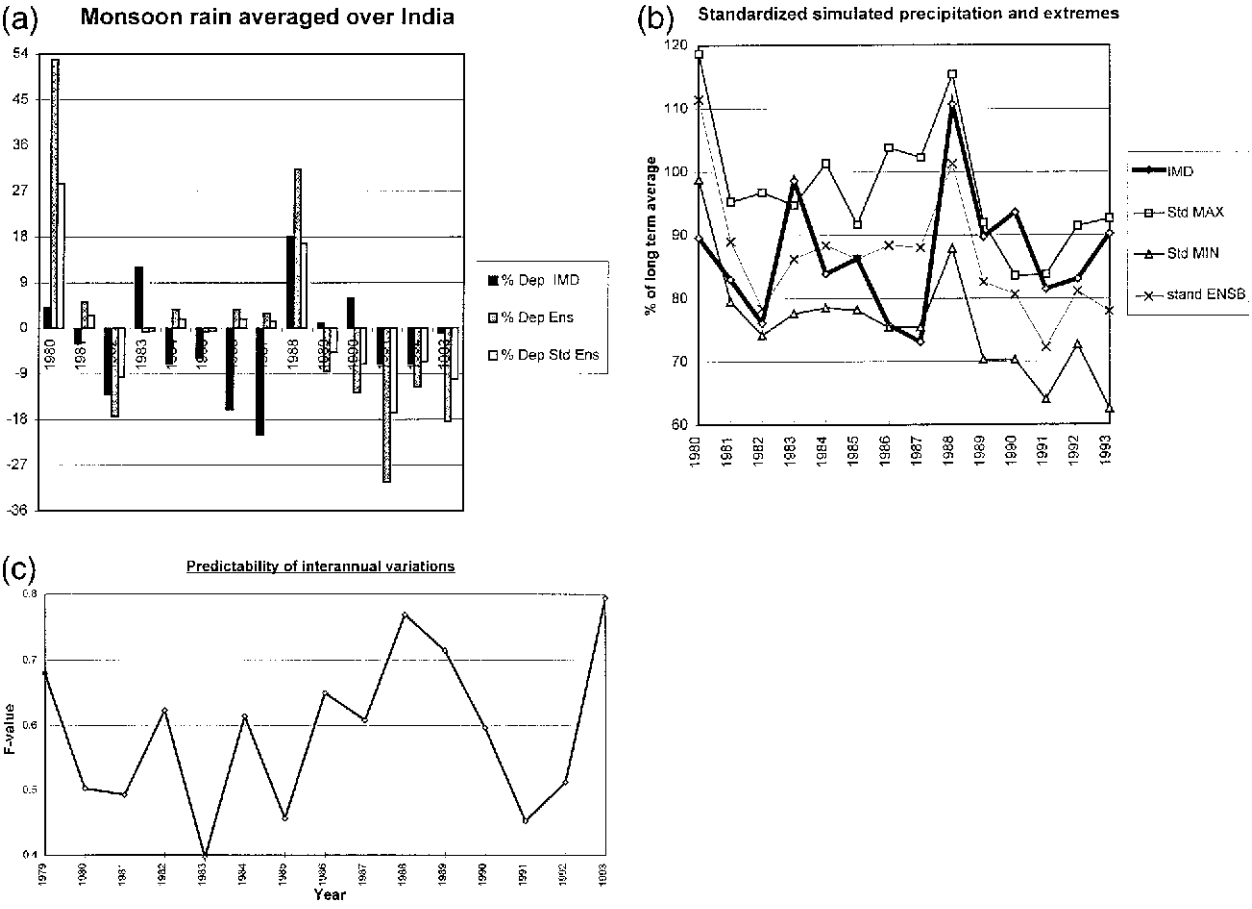

FIG. 5. (a) Percentage departure from the long-term mean of area-averaged precipitation over India as observed, as in ensemble average and standardized ensemble average. (b) Area-averaged seasonal total precipitation over India as percentage of long-term mean (IMD) against ensemble mean, ensemble maximum, and ensemble after standardization. (c) Predictability of interannual variability in the seasonal total area-averaged Indian precipitation.

mean and standard deviation as the observed precipitation. A comparison of the observed precipitation totals with the simulated values (Fig. 5b) shows that the mean simulation, in general, indicates the interannual trend and in most of the years the observed seasonal total precipitation lies within the bounds set by the maximum and minimum values realized in the ensemble. Since the number of members (9) in the ensemble is relatively small, it is reasonable to expect useful level of skill only in the simulation of seasonal total precipitation averaged over the whole of India. To demarcate the years with high-intrinsic predictability of interannual fluctuations, the ratio of the ensemble variance for a given year to the total variance from the set of all (135) simulations for the 15-yr period has been computed. This F value will be numerically small (C. Brankovic and T. N. Palmer 1998, personal communication) when the ensemble spread is small compared to the interannual variability of the ensemble mean. It is seen from Fig. 5c that the F value for Indian seasonal total rainfall is numerically small and does not exceed the value 1.0 during the 15-yr period under consideration. This indicates that the interannual variations in seasonal total have predictability.

The simulated intraseasonal variability in the Indian summer monsoon rainfall is studied by comparing the 10-day-accumulated values averaged over the 135 ensembles with the 15-yr average of the same quantity in the 1-day verifying analyses. It is seen from Fig. 6a that the accumulated rainfall over any 10-day period in a monsoon has a lower value in the simulation compared to the verifying. The observed weekly normal for India, computed by IMD from the 1901 to 1950 observations (Fig. 6b), cannot be compared directly with the verifying 1-day-predicted rainfall as the periods of accumulation and the area of space averaging are different. However, the highest rainfall rate of 8.88 mm day^{-1} predicted for the last decade of July agree well with the value of 9.90 mm day^{-1} observed during the eighth week of the monsoon (starting from 1 June). An averaging over a longer time period covering the highest rainfall epoch always produces a lower value.

The intraseasonal variability in precipitation reproduced in the verifying and seasonal simulations compare very well with the observed pattern that is essentially a trend increasing from the initial value of 2.3 mm day^{-1} in the first week of June to the maximum of 9.9 mm day^{-1} in the last week of July and then declining to 5.1 mm day^{-1} by the end of September. The spatial average value of precipitation is small in the beginning as during the ''onset'' phase of the monsoon and only a small part of the peninsular India experience rain while during July and August the whole of the country, except probably the extreme north, is under the spell of the monsoon. Again in September the monsoon current starts withdrawing from the west and the spatial average of rainfall starts decreasing. The normal values of weekly average precipitation rates do not indicate any specific period

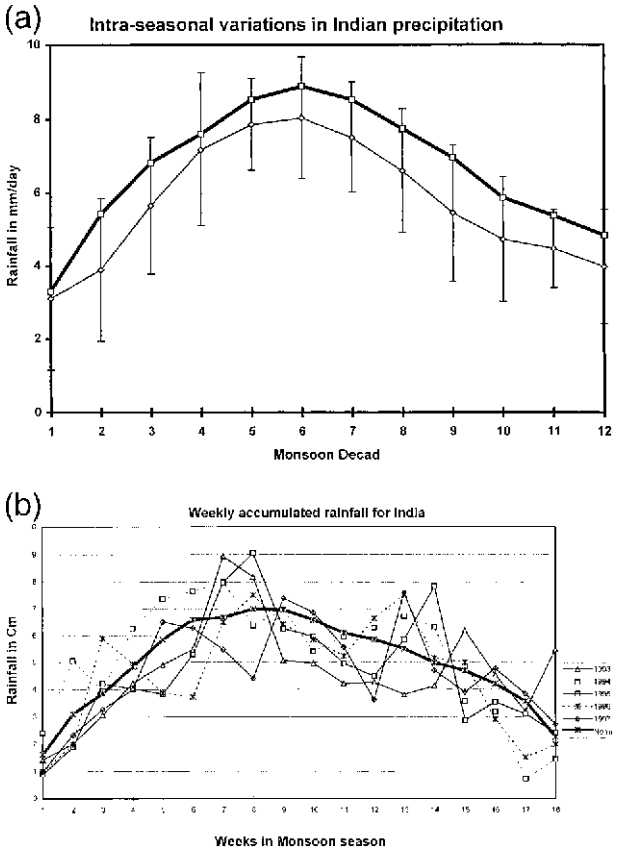

FIG. 6. (a) Intraseasonal variability in decadal precipitation averaged over India. Vertical bars represent ensemble standard deviation. (b) Weekly total precipitation for India as a whole computed from 1901 to 1950 observations. Also indicated are the actual values for years 1993–97. For operational purposes weeks are from Thursday to Wednesday.

over which the all-India rainfall has any significant departure from the trend. Also for the deficient years of 1979, 1982, 1986, and 1987 (or the excess years of 1983, 1988, and 1990), the 1-day verifying predictions do not indicate any specific temporal pattern except that a higher number of 10-day periods have less (or more) precipitation than the average. The 10-day accumulated precipitation values averaged over the 135 simulations show similar pattern as the verifying and normal values but have smaller magnitudes compared to the other two except for the first 10-day period when it exceeds the normal partly due to the longer period of averaging during the epoch of increasing trend in rainfall. As in the other two cases, no intraseasonal oscillation is seen in the ensemble mean of Indian rainfall.

The 10-day-average precipitation was subjected to the power spectrum analysis to determine whether any predominant periodicity, of more than 20 days (Sikka and Gadgil 1980), can be detected in the simulations. For the purpose of power spectrum analysis, the precipitation values were further averaged spatially over an area enclosing the normal location of the moist half of the

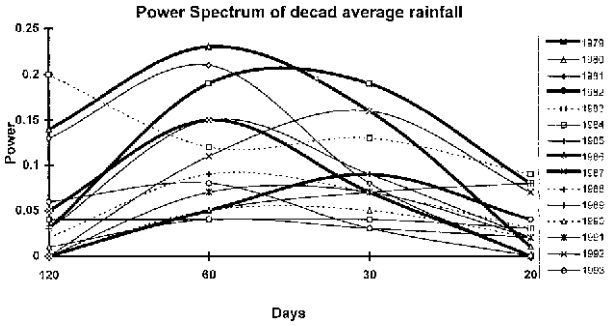

FIG. 7. Power spectrum of 10-day-average rainfall. Thick lines are for deficient monsoon years, dashed lines for good monsoon years, and the rest are for normal monsoon years.

monsoon trough. This choice of an averaging area, elongated in the E–W direction and of a shorter span in the N–S, would smooth out the effects of E–W modes but leave the N–S modes relatively unaffected. Each 10-day value in an ensemble was normalized by the seasonal average and then the mean over all the ensembles was taken to prepare the normalized decadal values for a particular year. These values were subjected to the power spectrum analysis to determine the distribution of power against the time period. It is seen from the plots (Fig. 7) that there is no district peak and no single dominant process can be isolated during the season that can lead to a clear periodicity in the 10-day-average precipitation. For a series of only 12 observations a power of less than 60% is not significant and it appears that the decadal average precipitation is a result of many N–S modes. All modes of the time period less than 20 days are filtered out by the 10-day averaging.

4. Distribution of other surface fields over India

The geographical distribution of the difference between the seasonal average of total cloud cover in the mean of 135 simulations and that in the mean 15-yr verifying 1-day prediction is shown in Fig. 8. Compared to the verifying 15-yr average of the 1-day predictions, the average seasonal simulation has less cloudiness along the west coast and up to the northwestern part of India while an area of excess cloudiness is seen over the northeastern part of the country extending into the Tibetan Plateau. The areas of deficit and excess cloudiness agree in general with the areas of deficit and excess rainfall, respectively. The areas of increase and decrease in soil moisture over the season broadly follow the precipitation pattern with on area of loss in soil moisture by more than 40 cm in the season around Gujarat, India.

The difference between the seasonal mean simulation and the verifying prediction of mean sea level pressure (Fig. 9) indicate slightly higher pressure over the sea areas adjoining India in the simulations while lower pressure prevails over the land. This pressure difference would lead to a anticyclonic anomaly in the lower-level

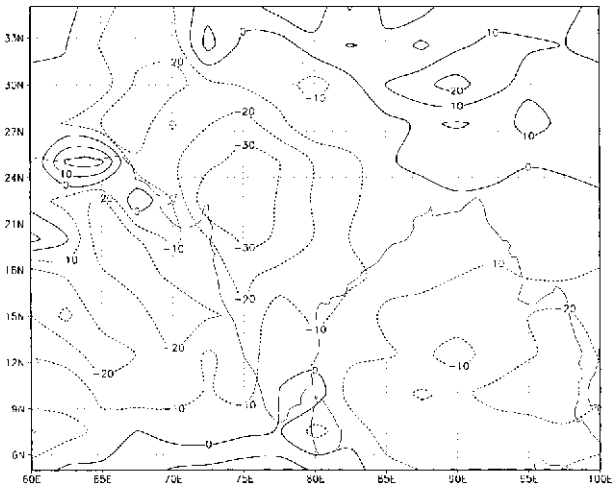

FIG. 8. Difference between the mean simulated and mean verifying 1-day total cloud cover (seasonal average) in percent.

wind over the sea areas introducing more northerly (along mountain) component in the predominantly westerly flow along the west coast and reducing the strength of easterly component in the southeasterly winds over the head bay. These differences in the wind field may explain the differences in the rainfall distribution at least partially.

The geographical distribution of the differences in the maximum and minimum temperatures at 2 m above ground between the mean simulated and mean verifying prediction (Figs. 10a,b) indicate that the near-ground atmospheric temperature over India has larger diurnal variation in the mean simulations with minimum temperatures lower by 4 to 6 degrees over most of the country while maximum temperatures are higher by 2 to 4 degrees. Comparison with observed (1951–80 mean) maximum and minimum temperature shows that

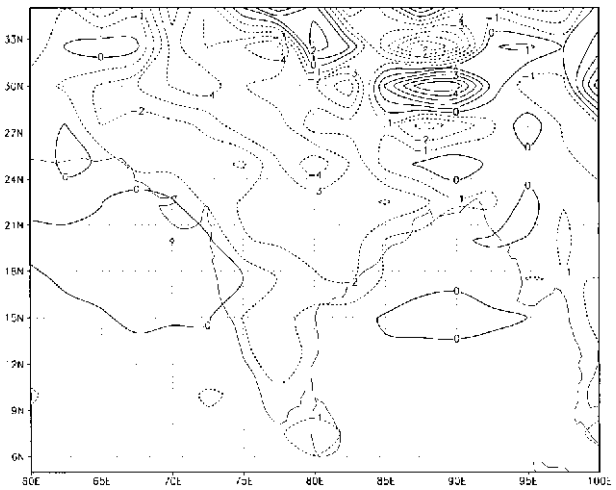

FIG. 9. Difference between the mean simulated and mean verifying 1-day mean sea level pressure (seasonal average; hPa).

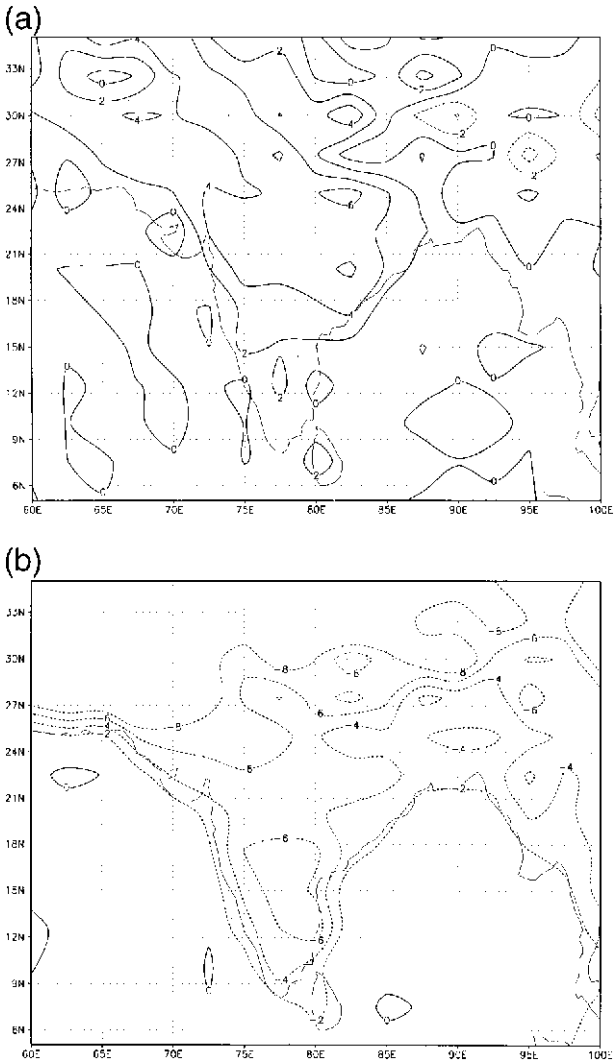

FIG. 10. (a) Difference between the mean simulated and mean predicted 1-day maximum temperature (seasonal average) in kelvins. (b) Difference between the mean simulated and mean predicted 1-day minimum temperature (seasonal average) in kelvins.

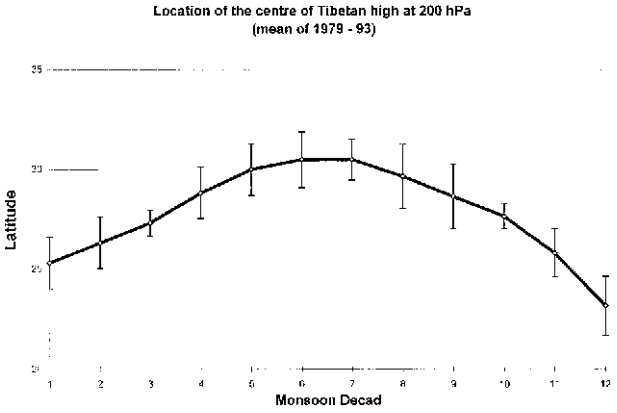

FIG. 11. Simulation of low-frequency variability during Indian summer monsoon—intraseasonal migration of the Tibetan anticyclone. The vertical bar is the magnitude of standard deviation during 1979–93.

simulated maximum temperatures are higher than that observed over central India while minimum temperatures are comparable. Higher maximum temperatures near the surface agree well with the lesser amount of cloud cover over central India.

In the global distribution (not shown) it is seen that the maximum temperature is higher than the corresponding value in the 1-day-verifying forecast over most of the land area by 2°C or more while the minimum temperature is lower over Asia and Australia with an area around the Tibetan Plateau where it is lower by more than 8°C. The amount of cloud cover may not be dominantly related to the 2-m temperature, as the simulated minimum temperature is significantly lower than the verifying temperature even over the area where the simulated cloud cover and precipitation are in far excess of the verifying values.

5. Simulation of upper-air features

During the summer monsoon season over India, specific patterns are seen in the mass and motion fields at the lower, mid-, and upper part of the troposphere. An important feature in the upper troposphere is the slow variation of the anticyclone that remains more or less anchored over the Tibetan Plateau during the months of July and August. The midlatitude westerly jet is located to the north of this anticyclone with a core at 200-hPa level, while the easterly jet, a typical feature of the Indian monsoon season, is located to the south of the anticyclone with the core at the 100-hPa level. During an active monsoon epoch, the anticyclone is located over the Tibetan Plateau as a single circulation between Arabia and southeast China, while during weak monsoon periods the circulation either breaks up into two connected cells, one to the east and the other to the west of the single cell center, or shrinks into a smaller circulation located over Arabia. A comparison of the number of ensemble members showing one of these two modes in the location of the anticyclone may provide a statistical measure of the probability of active monsoon over the central plains of India. The mean location of the center of the Tibetan high (Fig. 11), as obtained by averaging over the 135 ensembles spread over the 15 years, shows a slow northward movement initially up to the middle of July, stagnation around 30°N for about a month, and then a slow southward retreat up to 22°N by the end of September. The intensity of the anticyclone as indicated by the number of close contours around the circulation center, is maximum during the middle of August (not shown) when the circulation center is at its most northern position.

The latitudinal migration in the location of the center of the Tibetan high during the monsoon season shows

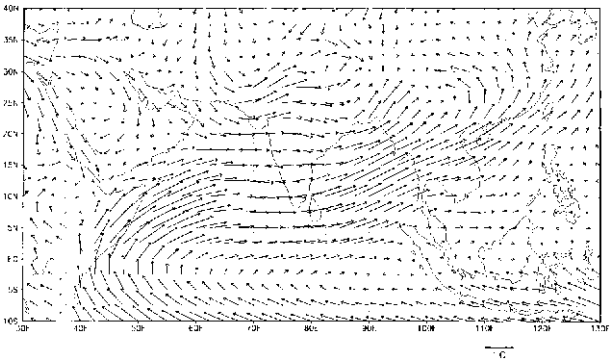

FIG. 12. Simulated summer monsoon flow over Indian region at 850 hPa (average of 135 ensembles over 15 yr) during the first decade of Jun.

considerable interannual variation (not shown) in the temporal sequence but traverses almost the same latitudinal band within the season. No distinct pattern in the temporal sequence could be discerned for the deficient or excess precipitation years.

The most typical feature of the Asian summer monsoon is the low-level wind flow over the north Indian Ocean and adjoining sea areas. The cross-equatorial flow to the east of Africa and southwesterly over the Arabian Sea and the Bay of Bengal are well reproduced at the 850-hPa level in the mean of the 135 simulations of the first 10-day period of the Indian summer monsoon (Fig. 12) spread over the 15 years of reanalysis. The band of weak easterly to the north of the line of wind turning (monsoon trough) over the central Indian plains is not prominent in the mean simulation and the moisture-laden wind appears to converge more to the east over the northeast of India and the adjoining southern parts of China. Also a wind trough with a north–south-oriented axis along 70°E is seen in the mean simulation to the west of India. Both these features, that is, the wind convergence over south China and the neighborhood and the trough to the west of India (north of 25°N) continue in mean simulations till the end of monsoon. The wind convergence region coincides with the region of excess precipitation in the simulations and indicates a locking of the principal component of precipitation due to the Asian monsoon to a ''break in monsoon'' scenario over India. The persistence of the north–south-oriented trough to the west of the northern parts of India throughout the monsoon season is an unusual feature produced possibly by the stronger daytime heating indicated by the higher (~6°C) maximum temperature in the mean simulation compared to the verifying simulation. A heat low type area of low pressure is located at the mean sea level just below the wind trough at 850 hPa.

During the Southwest monsoon season a strong south to north temperature gradient is present in the troposphere and the surface westerlies over India change into easterlies above 500 hPa. Below this level, convergence is associated with the monsoon flow while divergence is present above in association with the Tibetan anticyclone. Thus the vertical velocity field at 500 hPa is an indicator of the monsoon activity with respect to cloud (specially the convective cloud) formation and precipitation. The mean of the 1-day forecasts, averaged over the 15-yr reanalysis period, show a systematic intraseasonal change in the location and extent of the area of upward velocity. In the beginning of the season strong upward motion is noticed along the southern parts of the west coast of India and along the coast of Myanmar with a tongue of downward motion over the southwest bay in between. The subsidence over the western Arabian Sea is associated with the trade wind inversion. The plains of India to the north of 20°N are also under the grip of subsidence. As the season progresses the area under upward motion extends farther north and by the beginning of August (Fig. 13a) upward motion is present at 500 hPa over the whole of India, except the northwest part, with strong maxima over the west coast of India, the coast of Myanmar, and also the northeast of India indicating the presence of deep convection. Again at the end of the season an area of downward motion appears over the central plains of India at 500 hPa with weak upward motion confined to peninsular India and the coast of Myanmar. This intraseasonal variation agrees well with the onset, fully established, and retreat phases of the summer monsoon over India.

Computations of vertical velocity from observations are very few over the Arabian Sea and the Bay of Bengal as such observation are usually available only during special field campaigns like the Monsoon Experiment (MONEX). The presence of subsidence over the west Arabian sea during the Indian summer monsoon was detected (Ghosh et al. 1978) from the data collected by ships cruising across the Arabian Sea during MONEX-73. Subsidence over northwest India during the summer monsoon is a well-known fact confirmed by Das (1962) by numerical computations.

In the mean simulation the vertical velocity patterns are broadly similar but have a large difference in strength. During the established phase of the Southwest monsoon (Fig. 13b) upward velocities are much weaker over the west coast of India and the Myanmar coast but are stronger over Nepal and the adjoining areas to the east. The area of subsidence over the Southwest Bay of Bengal is stronger and more extensive during both the established and retreat phases.

6. Conclusions

The mean simulation of the Indian summer monsoon precipitation, as obtained by averaging the 135 seasonal realizations spread over the 15 years (1979–93) of the reanalysis period, shows distinct improvement over the earlier AMIP simulation. The land maximum over the west coast of peninsular India is now partially reproduced as an extension of the oceanic maximum over the

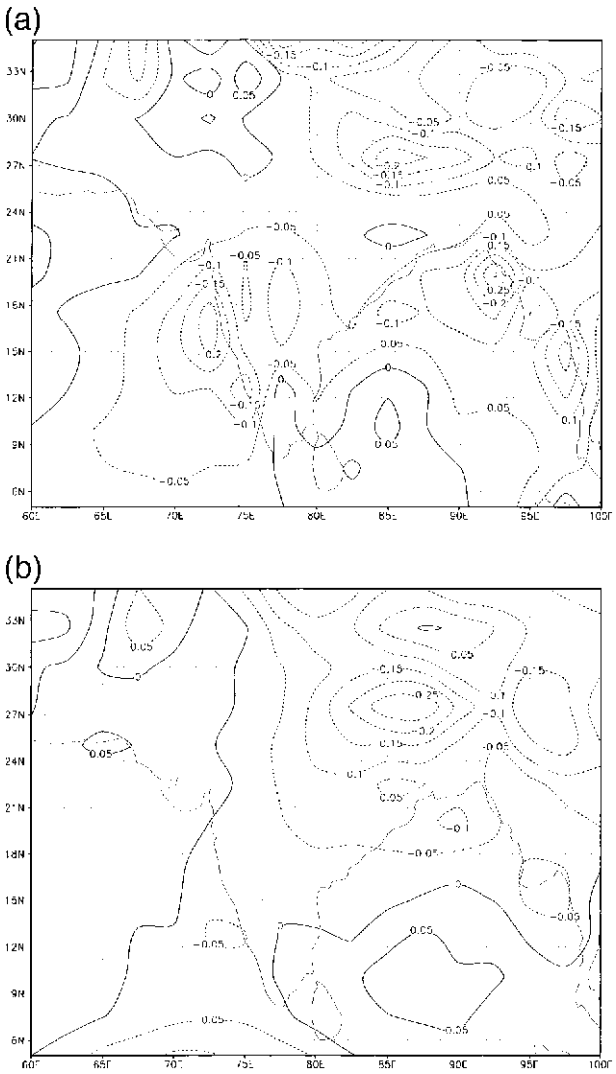

FIG. 13. (a) Simulated vertical velocity at 500 hPa in the mean (15 yr) 1-day predictions for the first decade of Aug. (b) Simulated vertical velocity at 500 hPa in the mean (135 ensembles) simulations for the first decade of Aug.

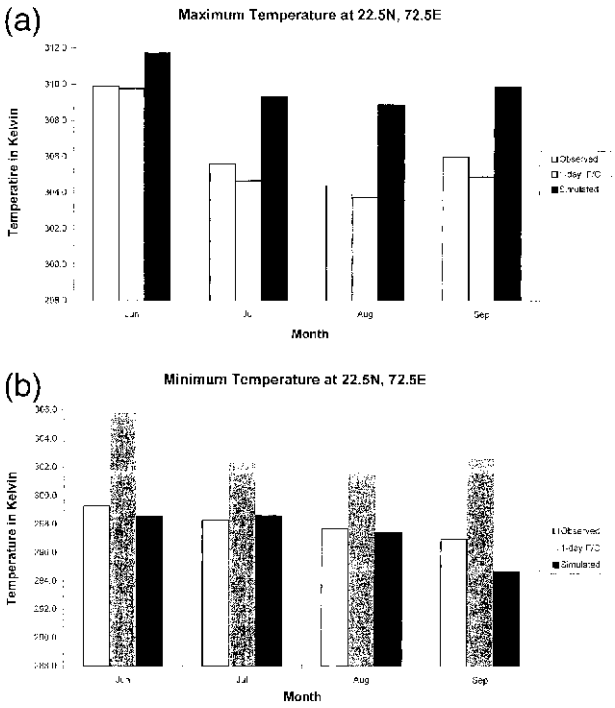

FIG. 14. (a) Comparison of monthly mean maximum temperature at a grid point over India. Observed value is the average of all station values (1951–80 normal) within the area bound by 21.25°–23.75°N and 71.25°–73.75°E. (b) Comparison of monthly mean minimum temperature at a grid point over India. Observed value is the average of all station values (1951–80 normal) within the area bound by 21.25°–23.75°N and 71.25°–73.75°E.

equatorial Indian Ocean. Higher resolution (T63L31) of the forecast model compared to that (T42L19) in the AMIP experiment, improved physical parameterizations, and better initial conditions are the main reasons for this improvement. Though the systematic error is still large in individual realizations, the interannual variability in the seasonal total of the spatial average Indian precipitation could be reproduced quite well in the ensemble means. A comparison of the ensemble spread with the interannual variability of the ensemble mean shows that the former is numerically smaller than the latter and the interannual variation in the seasonal total of the spatial averaged precipitation over India has predictability.

Examination of the 10-day averages did not indicate any distinct intraseasonal temporal pattern for the years of excess, normal, or deficient seasonal precipitation or any contrast between El Niño and La Niña years. No predominant mode with periodicity of more than 20 days could be isolated by the power spectrum analysis of the 10-day-average precipitation.

The diurnal maximum in the near-ground (2 m) air temperature is 2°–6°C higher (Fig. 14a) over India compared to the observed 30-yr mean (1951–80) for the whole of the monsoon season. The simulated monthly mean minimum temperature is closer to the observed (Fig. 14b) as compared to the 1-day mean forecasts in which the diurnal range appears to be very small. The mean sea level pressure in the simulation is lower over the Indian landmass and a trough in the westerly is seen at 850 hPa to the west of India, over the area of the largest rise in maximum temperature and the largest fall in mean sea level pressure.

The location of the Tibetan anticyclone at the 200-hPa level and its intraseasonal north–south migration is well reproduced in the seasonal simulation. Again no temporal pattern can be detected in the intraseasonal variability for the excess or deficient monsoon years.

To summarize, in the present seasonal simulations of the Indian summer monsoon by the ECMWF model, the distribution of the seasonal total precipitation is better than that in the AMIP simulations and the ensemble

spread is small enough for the interannual variability to have predictive value. The surface and upper-air fields examined are all consistent with each other and reflect most of the typical features associated with the Indian summer monsoon. The intraseasonal variability in the area-averaged seasonal precipitation and that in some of the slowly varying phenomena associated with the monsoon are also well reproduced in the seasonal simulations. However, the numerical values simulated for different meteorological fields correspond to a weak monsoon situation with significantly higher values of maximum temperature over central parts of India. No low-frequency (north–south) mode could be isolated from the Fourier analysis of 10-day-average precipitation.

Acknowledgments. The author is thankful to the director of ECMWF for providing the CD-ROM containing the seasonal simulations and to Drs. A. Hollingsworth, T. N. Palmer, and C. Brankovic of ECMWF for many helpful suggestions. The rainfall observation for India were provided by Dr. D. S. Upadhyay, director (Hydrology) of the India Meteorological Department (IMD). Dr. B. Mukhopadhyay, director in IMD has helped in the Fourier analysis of the 10-day averages of precipitation. Thanks are due to Dr. Kamal Puri of BMRC for encouraging the author to take up this work.

Some of the figures presented here have been drawn by using the GrADS plotting package provided by ECMWF with the data in the CD-ROM.

REFERENCES

Basu, B. K., K. J. Ramesh, and P. A. Harathi, 1999: Intercomparison of characteristic features of Southwest monsoon over India as reproduced in the mean monthly analyses and forecasts of some operational NWP centres in 1995. *Meteor. Atmos. Phys.,* **69,** 157–178.

Congbin, F., and J. Fan, 1984: Asian monsoon oscillations related and unrelated to the S. O. *Proc. VIII Annual Diagnostic Workshop*, WMO, 169–176.

Das, P. K., 1962: Mean vertical motion and non-adiabatic heat source over India during the monsoon. *Tellus,* **14,** 212–220.

Gadgil, S., S. Sajani, and participating AMIP Modelling Groups, 1998: Monsoon precipitation in AMIP runs. WMO/TD 837, 28 pp.

Ghosh, S. K., M. C. Pant, and B. N. Dewan, 1978: Influence of the Arabian sea on the Indian summer monsoon. *Tellus,* **30,** 117–125.

Hoinka, K. P., 1998: Mean global surface pressure series evaluated from ECMWF reanalysis data. *Quart. J. Roy. Meteor. Soc.,* **124,** 2291–2298.

India Meteorological Department, 1995: *Climatological Tables 1951–1980.* India Meteorological Department, 728 pp.

Kar, S. C., and B. K. Basu, 1992: Simulations of 1987 and 1988 summer monsoon with prescribed SST. *Proc. Conf. on Simulation of Interannual and Intraseasonal Monsoon Variability*, Boulder, CO, NCAR, WMO/TD 470, 2.79–2.86.

Palmer, T. N., C. Bronkovic, P. Viterbo, and M. J. Miller, 1992: Modelling interannual variations of summer monsoons. *Proc. Conf. on Simulation of Interannual and Intraseasonal Monsoon Variability*, Boulder, CO, NCAR, WMO/TD 470, 2.125–2.132.

Rao, Y. P., 1976: *Southwest Monsoon. Meteor. Monogr. on Synoptic Meteorology*, No. 1/1976, India Meteorological Dept., 337 pp.

Shukla, J., 1991: Short term climate variability and prediction. *Proceedings of the Second World Climate Conference*, J. Jager and H.L. Ferguson, Eds., Cambridge University Press, 203–210.

Sikka, D. R., and S. Gadgil, 1980: On the maximum cloud zone and the ITCZ over Indian longitude during the southwest monsoon. *Mon. Wea. Rev.*, **108,** 1840–1853.

Sperber, K. R., and T. N. Palmer, 1996: Interannual tropical rainfall variability in general circulation model simulations associated with the Atmospheric Model Intercomparison Project. *J. Climate*, **9,** 2727–2750.